Animal Cells and Systems
Vol. 14, No. 2, June 2010, 91–98

Taylor & Francis
Taylor & Francis Group

Temporal changes in mitochondrial activities of rat heart after a single injection of iron, including increased complex II activity

Misun Kim and Eunsook Song*

Division of Life Science, College of Natural Sciences, Sookmyung Women's University, Seoul 140-742, Republic of Korea

(Received 26 December 2009; final version received 14 April 2010)

Male rats were given a single injection of iron, and temporal changes in iron content and iron-induced effects were examined in heart cellular fractions. Over a period of 72 h, the contents of total and labile iron, reactive oxygen species, and NO in tissue homogenate, nuclear debris, and postmitochondrial fractions were mostly constant, but in mitochondria they continuously increased. An abrupt decrease in membrane potential and NAD(P)H at 12 h was also found in mitochondria. The respiratory control ratio was reduced slowly with a slight recovery at 72 h, suggesting uncoupling by iron. While the ATP content of tissue homogenate decreased steadily until 72 h, it showed a prominent increase in mitochondria at 12 h. Total iron and calcium concentration also progressively increased in mitochondria over 72 h. Enzyme activity of the oxidative phosphorylation system was significantly altered by iron injection: activities of complexes I, III, and IV were reduced considerably, but complex II activity and the ATPase activity of complex V were enhanced. A reversal of activity in complexes I and II at 12 h suggested reverse electron transfer due to iron overload. These results support the argument that mitochondrial activities including oxidative phosphorylation are modulated by excessive iron.

Keywords: iron overload; iron content; oxidative phosphorylation; mitochondria; reverse electron transfer; rat heart

Introduction

Iron is an essential micronutrient for aerobic organisms and is required for various oxido-reductive enzyme activities. Cellular iron is actively accumulated into mitochondria for the synthesis of heme and iron-sulfur centers for respiratory enzymes and enzymes of the tricarboxylic acid (TCA) cycle (Levi and Rovida 2009). Once processed, these iron complexes are redistributed from mitochondria into other parts of the cytoplasm (Napier et al. 2005; Rouault and Tong 2005). Disruption of transport and distribution can result in an excess or a lack of iron and may elicit pathological symptoms (Walter et al. 2002). Friedrich's ataxia, cardiopulmonary dysfunction due to hemochromatosis and thalassemia, and neurodegenerative diseases associated with aging are all linked to abnormal iron homeostasis (Lesnefsky 1994; Link et al. 1998; Brewer 2007).

Mitochondria, although primary sites of iron metabolism (Napier et al. 2005), can be readily injured by excessive iron. Virtually all kinds of mitochondrial macromolecules suffer from oxidative damage (Britten et al. 2002). The electron transport chain serves as an effective machinery of reactive oxygen species (ROS) generation, in which complex I and/or complex III are major sites of superoxide production (Brand et al. 2004). Iron is active in ROS production, but the specific details associated with the physiological role of iron metabolism are currently unknown.

Previous studies have revealed deleterious effects of iron overload on mitochondria in rat tissues (Kim et al. 2008, 2009). To determine the primary step that is affected by iron, it is necessary to investigate time-dependent changes. In this study, mitochondrial parameters and iron-related factors such as ROS and NO were traced over a 72-h period following a single injection of iron.

Materials and methods

Animal treatment and injection of iron

Male Sprague-Dawley rats were obtained from Orient Biology Inc. (Korea). All groups were raised in the same facility and received the same diet (Purina Mills) and water ad libitum as previously described (Kim et al. 2009). Male rats (260–280 g) were injected hypodermically with $FeCl_3$ (0.049 mg/g). After injection, rats were sacrificed at the indicated time during a 72-h period. For the control, phosphate-buffered saline (PBS) was used in place of $FeCl_3$ under the same conditions.

Isolation of heart mitochondria

Hearts were perfused with PBS with heparin (500 U/kg), quickly excised, washed with 0.25 M cold sucrose

*Corresponding author. Email: eunsong@sookmyung.ac.kr

ISSN 1976-8354 print/ISSN 2151-2485 online

DOI: 10.1080/19768354.2010.486936
http://www.informaworld.com

solution, and chopped into small pieces in isolation buffer (0.25 M sucrose, 20 mM Tris-Cl, pH 7.4, 1 mM EDTA, 1 mM EGTA), containing 0.5% protease inhibitor cocktail (Sigma), 10 mM NaF, 1 mM Na_3VO_4. Minced tissues were incubated for 5 min with 0.05% saponin and homogenized loosely with a glass homogenizer, followed by rough homogenization with Teflon (Pande et al. 1971). The homogenate was centrifuged at $10,000 \times g$ for 20 min at 4°C, and the pellet was suspended in isolation buffer, washed twice, and kept at −80°C until use. The homogenate was centrifuged at $2000 \times g$ for 20 min at 4°C and following two fractions were separated. The pellet was suspended in isolated buffer, washed twice, and kept at −80°C until use for the fraction of nuclear debris. The supernatant was further centrifuged at $10,000 \times g$ for 20 min at 4°C. The resulting supernatant was used for postmitochondrial fraction. The pellet was suspended in isolation buffer, washed twice, and kept at -80°C until use for mitochondria.

Determination of iron and calcium contents, ROS, NO, NAD(P)H, and ATP

Total iron content was measured according to Levi et al. (1988). Prepared samples (250 μg) were added to 1 ml of 25 mM $NaSO_4$, 0.01% (v/v) bipyridyl, and 10% (v/v) acetic acid. After boiling for 90 min, the mixture was cooled and centrifuged. The absorbance of the supernatant was measured at 520 nm with a UV 2550 double-beam spectrophotometer (Shimazu, Japan). For measurement of labile iron content, prepared samples (100 μg) were suspended into 1 ml phosphate-buffered saline (PBS) and 500 nM calcein was added immediately (Invitrogen, USA). After 5 min, the fluorescence was measured at 495 nm (excitation) and 517 nm (emission) with a JA-750 fluorometer (Jasco, Japan). Because fluorescence of calcein was quenched by bound iron, labile iron content was measured in the absence and presence of iron.

Total mitochondrial calcium was determined using 40 μM Arsenazo III (Sigma) in PBS (Gorman et al. 1978). The concentration was measured by standard curve using a standard $CaCl_2$ solution.

Reactive oxygen species (ROS) content was measured as described by Valkonen et al. (1997). Prepared samples (~250 μg) were suspended in 1 ml of PBS (pH 7.4), mixed with 330 μM of 2′7′-dichlorodihydrofluorescein (DCF) diacetate, and the relative absorbance was estimated at 504 nm.

NO was measured according to Kolb et al. (1994). Prepared samples (500 μl at 0.25 mg/ml) were mixed with an equal amount of Griess reagent containing 0.1% *N*-(1-naphthyl)ethylenediamine and 1% sulfanilamide for 10 min at 4°C. Absorption was measured at 550 nm.

For NAD(P)H quantitation (Masini et al. 1987), 250 μg of mitochondria was suspended in 1 ml PBS and fluorescence was compared at 340 nm (excitation) and 465 nm (emission) by a JA-750 fluorometer (Jasco, Japan).

Total ATP content (Lundin et al. 1975) was determined using a luminescence kit (Promega, USA) and luminometer (Berthold technology, USA) following the manufacturer's instructions.

Measurement of RCR and membrane potential

The respiratory control ratio (RCR) of isolated mitochondria was determined according to Estabrook (1967). Isolated mitochondria were suspended to 1 mg/ml in 0.25 M sucrose, 20 mM Tris-Cl (pH 7.4), 5 mM $MgCl_2$, 20 mM KCl, and 1 mM EDTA. The suspension was incubated in an oxygen chamber at 25°C with circulating water. After 30 s, 10 mM glutamate and 5 mM malate were added as substrates of complex I (state 2). Then, 1 mM ADP was added (state 3) and the oxygen consumption was monitored. The oxygen curve stabilized after a few minutes (state 4). RCR was calculated as the ratio of oxygen consumption at state 3 to that at state 4.

For measurement of the mitochondrial membrane potential, 10 nM rhodamine 123 was added to 0.25 mg/ml mitochondrial suspension according to the method of Emaus et al. (1986). Changes in the potential were measured by the decrease of fluorescence at 503 nm (excitation) and 533 nm (emission). The fluorescence was normalized using 1 μM CCCP.

Measurement of enzyme activities of mitochondrial electron transport system, from complex I to complex V

Enzyme activity was determined by the method of Barrientos (2002). For the rotenone-senstive NADH-decylubiquinone oxidoreductase (complex I), 800 μl of H_2O was added to 40 μg mitochondria and incubated for 2 min at 37°C. Tris-Cl (200 μl, 50 mM, pH 8.0) supplemented with 5 mg/ml BSA, 0.8 mM NADH, 240 μM KCN, and 4 μM antimycin A was added and the reaction was started with 50 μM of 2,3-dimethoxy-5-methyl-6-*n*-decyl-1,4-benzoquinone. After 3 min, the reaction was detected by absorbance at 340 nm. Rotenone (4 μM) was added to measure rotenone-sensitive activity. Succinate:ubiquinone reductase (complex II) activity was assayed from the reduction of 2,6-dichlorophenolindophenol (DCPIP). Mitochondria (40 μg) were added to 1 ml of 10 mM KH_2PO_4 (pH 7.8), 2 mM EDTA, 1 mg/ml BSA, 4 μM rotenone, 0.2 mM ATP, and 80 μM DCPIP as an acceptor. The mixture

was preincubated for 10 min at 30°C in the presence of 10 mM succinate and the reaction was started by addition of 80 μM decylubiquinone. The activity was measured at 600 nm for 5 min. The mixture including 10 mM malonate was used as a negative control.

The activity of ubiquinol cytochrome c reductase (complex III) was performed at 550 nm following the increase in absorbance resulting from the reduction of cytochrome c. Total reaction volume was 1 ml containing 10 mM KH_2PO_4 (pH 7.8), 2 mM EDTA, 1 mg/ml BSA, mitochondria (40 μg), 80 mM decylubiquinol, 240 μM KCN, 4 μM rotenone, and 200 μM ATP. The reaction was started by the addition of 40 μM oxidized cytochrome c and measured for 5 min. The addition of 0.4 μM antimycin A allowed us to distinguish between the reduction of cytochrome c catalyzed by complex III and the nonenzymatic reduction of cytochrome c by the reduced quinone. Cytochrome c oxidase (complex IV) assay was performed at 550 nm following the decrease in absorbance resulting from the oxidation of reduced cytochrome c. Mitochondria (40 μg) and 10 μM reduced cytochrome c (by addition of sodium dithionite) were added to 1 ml of isosmotic medium containing 10 mM KH_2PO_4 (pH 6.5), 0.25 M sucrose, and 1 mg/ml BSA.

Oligomycin-sensitive ATPase (complex V) was measured spectrophotometrically by a coupled assay using lactate dehydrogenase and pyruvate kinase as the coupling enzyme. The measurement was performed at 340 nm following the decrease in absorbance resulting from NADH oxidation. Mitochondria (40 μg in H_2O) were incubated at 37°C for 30 s and added to 200 μl of medium (warmed at 37°C for 5 min) containing 50 mM Tris-Cl (pH 8.0), 5 mg/ml BSA, 20 mM $MgCl_2$, 50 mM KCl, 15 μM carbonyl cyanide *m*-chlorophenylhydrazone (CCCP), 5 μM antimycin A, 10 mM phosphoenolpyruvate (PEP), 2.5 mM ATP, 4 units each of lactate dehydrogenase and pyruvate kinase, and 1 mM NADH. The oxidation of NADH was monitored for 3 min at 340 nm. Then, 3 μM oligomycin was added and the reaction was followed for an additional 3 min to distinguish the ATPase activity coupled to the respiratory chain. For normalization of oxidative phosphorylation activity, citrate synthase activity was assayed as previously described (Barrientos 2002). The absorbance was measured at 412 nm following the reduction of 0.1 mM 5,5′-dithiobis(2-nitrobenzoic acid) in the presence of mitochondria (40 μg), 0.2 mM acetyl-CoA in 10 mM Tris-HCl (pH 7.5), and 0.2% Triton X-100. The baseline was maintained for 5 min, and the reaction was started by the addition of 0.5 mM oxaloacetic acid.

Results

Changes in iron, NO, ROS, and ATP in the cellular fractions

Following a single injection of iron, heart tissue from rats was collected at 12, 24, 48, and 72 h and the effects of the iron were studied in various cellular fractions after assessment of each fraction using typical markers (Figure 1A). Labile iron in the tissue homogenate increased sharply at 24 h, decreased at 48 h, and increased again at 72 h (Figure 1B). This cyclic pattern also occurred in the nuclear debris, with a quick increase as early as at 12 h. The labile iron content of mitochondria fell at a constant rate until 24 h, but increased abruptly from 48 h until 72 h. The total iron of the tissue homogenate steadily increased during the 72-h period, slowing after 48 h (Figure 1C). A rapid increase of total iron was observed in the mitochondrial fraction, with a sharp increase at 48 h. An abrupt increase in total iron was also found at 12 h in the nuclear debris. In the postmitochondrial fraction, total iron was significantly higher at 48 h in contrast with the constant level of labile iron. These results suggest that labile iron distributes itself among various organelles in the cell and that there is a different temporal sequence in each cellular fraction. Thus, the nuclear debris exhibited an immediate rise in both labile and total iron, while the labile iron concentration in mitochondria was initially low. Newly imported iron may stay in or around the plasma membrane (collected as nuclear debris) until its fate within the cell is determined (Muñoz et al. 2009). The total iron content of the mitochondria and homogenate showed a steady increase indicating that some of the iron may associate with the components of redox enzymes. From 24 h to 48 h, labile iron was diminished in the nuclear debris but augmented markedly in the mitochondria, and similar changes were found for total iron. The progressive marked increase of both labile and total iron in mitochondria at 72 h is in accordance with the role of mitochondria as a major reservoir of excessive iron. The initial barrier to iron transport set up by the plasma membrane results in increased labile iron in the nuclear debris fraction, but over time some of the imported iron is transported into mitochondria for processing into iron complexes, such as heme and iron-sulfur centers (Lill et al. 2006). These iron complexes should be utilized mostly for mitochondrial components and various cellular compartments (Atamna et al. 2002), with excessive labile iron stored in the mitochondria. This labile iron appears to be associated with nitric oxide (NO), a well-known iron binding compound that inhibits enzymes of the oxidative phosphorylation system (Chénais et al. 2002).

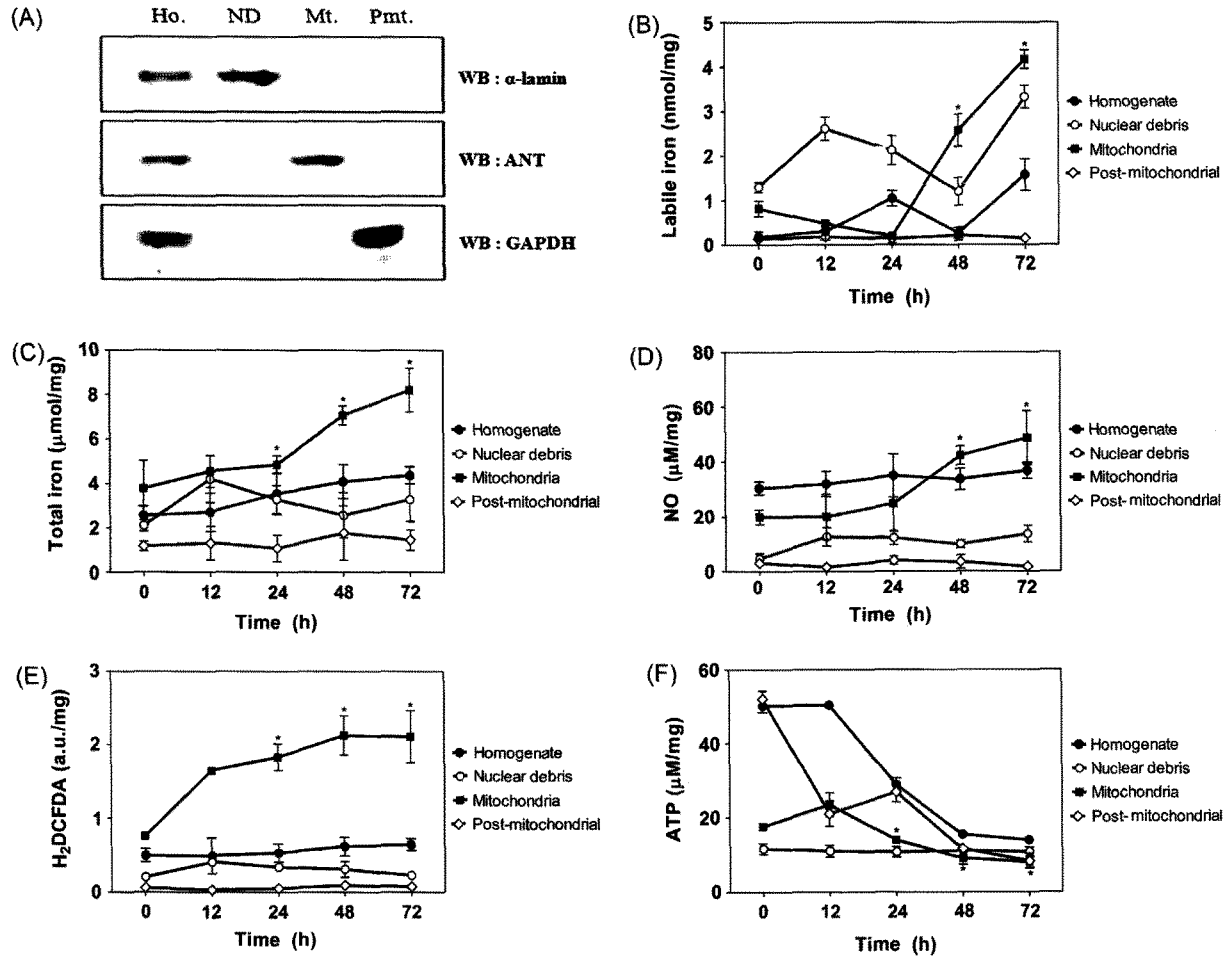

Figure 1. Fractionation of heart homogenate and change of iron content, ROS, NO, and ATP after single injection of iron in rats. To trace iron effect, a single hypodermic injection of FeCl3 was given. Heart was excised after 12, 24, 48, and 72 h, for preparation of homogenate (closed circle), nuclear debris (open circle), mitochondria (closed square) and post-mitochondrial fraction (open diamond) by differential fractionation. These fractions were used for the measurement of iron content, ROS, NO, and ATP as described in Materials and methods. (A) Western analysis of heart homogenate (Ho.) which was fractionated into nuclear debris (ND), mitochondria (Mt.), and postmitochondrial fraction (Pmt.) with α-lamin, adenine nucleotide translocase (ANT), and alpha-glyceraldehyde dehydrogenase (GAPDH), respectively. (B) Labile iron, (C) total iron, (D) nitric oxide (NO), (E) reactive oxygen species (ROS) in arbitrary units (a.u.), and (F) ATP. *For (C) through (F), $P < 0.01$, and for (B), $P < 0.0001$, compared with control (0 h). Data are presented as mean ± SD of 20 separate experiments.

In this study, NO increased progressively in mitochondria with a sharp rise at 48 h similar to total iron (Figure 1D). In the nuclear debris, NO rose rapidly at 12 h similar to labile iron. This parallel response suggests that nitric oxide synthase (NOS) on/near the plasma membrane generates NO for imported/released iron (Watts et al. 2003; Richardson et al. 2008). A similar change in NO and labile iron was observed for mitochondria at 48 h, suggesting that mitochondrial NOS may act as a protective blockade against the devastating effect of iron.

Reactive oxygen species (ROS) increased in the mitochondria until 48 h, with a sharp rise at 12 h (Figure 1E). There were only slight changes in the homogenate, nuclear debris, and postmitochondrial fractions. Although labile iron is thought to stimulate ROS production (Harley et al. 1993), in this study ROS was more closely associated with total iron in the mitochondria. Presumably, iron processing in the mitochondria relies on some unknown activity that generates ROS, and labile iron may become total iron, limiting the amount of free iron to a narrow range. Based on the severe drop in membrane potential and NAD(P)H at 12 h (Table 1), this activity appears to be related to electron transport (Table 2). The rapid responses of membrane potential, NAD(P)H, and ROS generation imply that mitochondrial activity is directly involved in iron metabolism.

Change in ATP content contrasted with change in total iron (Figure 1F). At 12 h, ATP of tissue

Table 1. Effect of iron on respiratory chain ratio (RCR), membrane potential, content of NAD(P)H and calcium of mitochondria after single injection of iron.

Time (h)	RCR(ADP/O)	Membrane potential (a.u./mg)	NAD(P)H (a.u./mg)	Ca^{2+} (nmol/mg)
0	6.26±0.52	369±14.04	336±45.01	6.31±0.52
12	5.97±2.18	241±54.67	129±14.73	7.94±0.87
24	5.04±1.02*	220±42.34	116±21.07*	9.63±1.93
48	4.01±0.83*	268±36.37*	121±06.03*	11.77±3.52*
72	4.25±1.24*	269±04.59*	143±20.21*	12.21±2.77*

Data are presented as mean ± SD from 20 independent experiments. Arbitrary unit of fluorescence is taken as a.u. *P <0.001 compared with control (0 h).

homogenate remained constant, while a significant increase was seen in mitochondria with a concomitant drop in the postmitochondrial fraction. Interconversion of ATP with creatine phosphate from the postmitochondrial fraction may supply mitochondrial energy needs (Balaban 2009). This trend is reversed at 24 h, indicating that energy loss originated from inhibited oxidative phosphorylation in iron-affected mitochondria. In particular, the low level of labile iron at 12 and 24 h suggests active sequestration through formation of unknown iron complexes. At 48 h, iron concentration appears to exceed the manageable limit of the mitochondria, resulting in an increase in labile iron. In contrast, the cyclic pattern seen in other fractions implies a passive role in iron management.

Changes in calcium content, NAD(P)H, RCR, and membrane potential of mitochondria

The marked change in mitochondrial iron concentration led us to examine mitochondrial activity (Table 1). The calcium content of mitochondria increased in parallel with iron increase during a 72 h-period after iron injection. Calcium appears to be one target of iron, allowing iron to exert its effects through changes in calcium concentration. Iron affects calcium mobilization, especially through mitochondria (Romslo and Flatmark 1973; Gogvadze et al. 2002).

Mitochondrial reducing power, NAD(P)H, and membrane potential showed a marked drop at 12 h (down to 35% at 24 h) with slight elevation at 48 h and incomplete recovery at 72 h (43%) (Table 1). Iron is transported as ferrous ion in most cases and a reducing agent is necessary. NAD(P)H in mitochondria, a major source of reducing power for cellular redox activities, provides a fundamental reduction source for iron transport. In addition, removal of ROS depends ultimately on this reduction potential (Ying 2008). Oxidative pathways in mitochondria can supply NAD(P)H, but if consumption is higher than production, supplementary pathways may operate. NAD(P)H may be produced by harnessing the respiratory chain through reverse electron transfer by sacrificing membrane potential. The peculiar augmentation of complex II activity found in this study (Table 2) supports this alternate pathway. RCR was low during this period, which was least at 48 h (64% of 0 h) with slight recovery at 72 h (68% of 0 h). In the presence of iron as an uncoupler (Vatassery 2004), normal levels of state IV may not be attained due to low levels of ATP. The resulting high levels of ADP yielded low RCR. Iron uptake by mitochondria may be attributed to low RCR, as ATP is consumed via the ATPase activity of complex V.

Diminished membrane potential was also observed as early as 12 h, with a minimum at 24 h. These simultaneous changes in reducing power and membrane potential imply an association with the modulating events of mitochondrial iron metabolism. Membrane potential recovered slightly at 48 h, reaching a plateau until 72 h (73% of 0 h). Compared to RCR, membrane potential showed an earlier decline.

Table 2. Effect of iron on the enzymatic activity of oxidative phosphorylation after single injection of iron.*

Time (h)	Complex I	Complex II	Complex III	Complex IV	Complex V
0	35.26±0.10	13.46±0.12	19.42±0.01	25.27±0.19	24.02±0.52
12	37.64±0.01	13.21±0.24	18.08±0.26	20.84±0.15	25.21±0.18
24	27.95±0.02	14.61±0.09	17.27±0.35	16.37±0.75	27.66±0.23
48	23.91±0.04	15.45±0.13	15.15±0.01	12.75±1.04	30.89±0.02
72	22.75±0.04	17.92±0.37	14.87±0.21	12.88±0.35	33.35±0.78

Enzyme activity is shown in μM/mg per min. After a single injection of iron, rats were sacrificed after various times (h) and enzyme activities of complex I to complex V were measured as described in Materials and methods. Data are presented as mean ± SD from 18 independent experiments. *P <0.01 compared with control (0 h), all results were significant.

As iron uptake into mitochondria depends on membrane potential (Romslo 1975), the early abrupt fall of membrane potential supports the critical role of mitochondria in iron sequestration. NAD(P)H is the ultimate reducing power for the elimination of ROS and sharp changes in these factors at 12 h are consistent with iron related events occurring in mitochondria at that time. The considerable increase of ROS at 12 h may be responsible for the dramatic loss of reducing power during the same period. The later recovery of reducing power and membrane potential are crucial for cellular activities and survival.

Change of oxidative phosphorylation activity by iron

Iron is actively transported into mitochondria primarily to synthesize heme and iron-sulfur centers essential for respiratory enzyme complexes I through IV. To examine the effect of iron on oxidative phosphorylation, enzymatic activities of complexes I through V were measured. Overall activities of complexes I, III, and IV steadily decreased over a 72-h period, whereas those of complexes II and V increased (Table 2). A marked fall in complex IV activity (49% decrease) was noted, confirming previous studies (Atamna 2004; Kim et al. 2009).

Enhanced ATP hydrolysis following iron injection may be associated with the abrupt fall in membrane potential that occurred during the early phase. Compared to the expected high ATPase activity of complex V that maintains membrane potential in response to iron overload (Machida and Tanaka 1999), the increase in complex II activity was puzzling. Interestingly, complex I activity rose at 12 h, while complex II activity fell. After 24 h, the activity of complex I dropped but that of complex II escalated, implying reverse electron transfer (Vinogradov and Grivennikova 2005).

Discussion

Cyclic change of labile iron content prominent in nuclear debris suggests that membranous structure such as plasma membrane may be the natural entry point of labile iron. Rather slow change of labile iron in mitochondria may be related to slight increase of total iron in mitochondria. Possibly imported labile iron is rapidly taken up by nearby mitochondria and subsequently incorporated into iron complexes such as heme and iron sulfur center. The continual increase of total iron content of mitochondria differed from the constant, slightly periodic, pattern in other cellular fractions. This persistent iron loading implies that mitochondria may be the control center for modulating excess iron and related events similar to their roles for calcium homeostasis (Graier et al. 2007). The accumulation of iron in mitochondria may initiate paracrystalline inclusions found in patients of myopathy under the electron microscope (Hulsmann et al. 1967).

Membrane potential, RCR, and contents of calcium and NAD(P)H of mitochondria are compromised as early as 12 h, consistent with changed iron content. Early change of these foremost factors of mitochondria supports our argument that iron plays crucial role in determining mitochondrial activity. One way could be through calcium as calcium level affects mitochondrial activity (Lehninger 1970; Feissner et al. 2009). One effect is augmentation of NAD(P)H to remove ROS via calcium-dependent activation of the TCA cycle (Feissner et al. 2009; Liu and O'Rouke 2009). Iron-induced depolarization may activate calcium input, facilitating energy supply by the TCA cycle via oxidative phosphorylation. Intracellular calcium also activates mitochondrial ATP synthase in rat heart (Das and Harris 1990; Territo et al. 2000). Though increased calcium in mitochondria in the presence of excessive iron cannot be explained, ROS may cause calcium change (Csordás and Hajnóczky 2009). A notable consequence of calcium is increased activation of enzymes in the TCA cycle producing NAD(P)H (Hansford and Zorov 1998). A consequence of augmented NAD(P)H via calcium-dependent activation of the TCA cycle may contribute to removing ROS (Feissner et al. 2009; Liu and O'Rouke 2009). Our experiments on the oxidative phosphorylation system caused by excess iron revealed an immediate (and probably direct) decrease in NAD(P)H and membrane potential with parallel decreases in complex I, III, and IV with rescuing activities of complex V and II. We propose that NAD(P)H is used directly for reducing iron for transport into mitochondria and/or for synthesis of heme and iron-sulfur centers. Thus, during iron transport, NAD(P)H oxidation by the electron transport chain may be suppressed by direct inhibition of respiratory complexes by NO, or by iron itself, resulting in the ablation of membrane potential. Complex V, in turn, may be activated to restore membrane potential. In addition, reverse electron transfer operated by complex II may be responsible for altered OXPHOS activity, as observed in this investigation.

Iron affects respiratory chains in heart mitochondria and an impaired oxidative phosphorylation system generates ROS (Link et al. 1998). Iron stimulates NO production in mitochondria through mtNOS (Kanai et al. 2001), leading to inhibition of respiratory chains, including complex II (Pearce et al. 2009). NO specifically binds and inhibits complex IV (Brown and Cooper 1994; Giuffrè et al. 1996), and complexes III and I, contributing to reduction of the membrane potential. Breakdown of NO by complex IV (cytochrome c oxidase) may lead to subsequent loss of the enzyme activity (Cooper 2002). Alternatively, iron may

be oxidized directly by complex IV as postulated in bacteria, with uncoupling-like results (Castelle et al. 2008).

Reverse electron flow occurs through complex II via succinate to complex I to produce NADH (Chance and Hollunger 1961). Complex I can undergo conformational change depending on the relative amount of NAD^+ versus NADH to facilitate reverse electron transfer from complex II (Grivennikova et al. 2007). Thus, complex II links the TCA cycle to complex III of the electron transport chain and simultaneously restores reducing power to complex I, which was lost during the elimination of ROS caused by excessive iron. Reverse electron transfer can maintain reduction potential critical for cell survival (Ying 2008). A substantial increase in complex II could supply electrons through split pathways, one upstream to complex I, the other downstream to complex III. Through complex I, reducing power would be generated as NADH, while normal electron transport downstream would support membrane potential and ATP production. Under the present condition, elevated activity of complex II and the high ATPase activity of complex V may be required to restoring the membrane potential critical to cell survival (Mao et al. 2007).

The present study clearly shows that a single injection is sufficient to investigate iron-related changes in heart mitochondria. Increased iron content resulted in increased calcium concentration, ROS, and NO, which are directly related to the respiratory activity of mitochondria. Interestingly, the effect of iron on mitochondria resembled the effect of calcium. Membrane potential, RCR, and NAD(P)H, which are typical integrative parameters of mitochondrial activity, decreased substantially. Likewise, respiratory enzyme activities declined, except complex II. Notably, enhanced activity of complex II implies the possible existence of an alternative pathway, and further studies are indicated.

Acknowledgements

This work was supported by the SRC/ERC program (2009) of the Korea Science and Engineering Foundation (KOSEF) through the Research Center for Women's Disease (RCWD) at Sookmyung Women's University and by the Seoul Research and Business Development Program and also by the Seoul R&BD program (no. 10582).

References

Atamna H. 2004. Heme, iron, and the mitochondrial decay of ageing. Ageing Res Rev. 3:303–318.

Atamna H, Walter PB, Ames BN. 2002. The role of heme and iron-sulfur clusters in mitochondrial biogenesis, maintenance, and decay with age. Arch Biochem Biophys. 397:345–353.

Balaban RS. 2009. Domestication of the cardiac mitochondrion for energy conversion. J Mol Cell Cardiol. 46:832–841.

Barrientos A. 2002. In vivo and in organello assessment of oxphos activities. Methods. 26:307–316.

Brand MD, Affourtit C, Esteves TC, Green K, Lambert AJ, Miwa S, Pakay JL, Parker N. 2004. Mitochondrial superoxide: production, biological effects, and activation of uncoupling proteins. Free Rad Biol Med. 37:755–767.

Brewer GJ. 2007. Iron and copper toxicity in diseases of aging particularly Atherosclerosis and Alzheimer's Disease. Exp Biol Med. 232:323–335.

Britton RS, Leicester KL, Bacon BR. 2002. Iron toxicity and chelation therapy. Int J Hematol. 76:219–228.

Brown GC, Cooper CE. 1994. Nanomolar concentrations of nitric oxide reversibly inhibit synaptosomal respiration by competing with oxygen at cytochrome oxidase. FEBS Lett. 356:295–298.

Castelle C, Guiral M, Malarte G, Ledgham F, Leroy G, Brugna M, Giudici-Orticoni M. 2008. A new iron-oxidizing/O_2-reducing supercomplex spanning both inner and outer membranes, isolated from the extreme acidophile *Acidithiobacillus ferrooxidans*. J Biol Chem. 283:25803–25811.

Chance B, Hollunger G. 1961. The interaction of energy and electron transfer reactions in mitochondria I. General properties and nature of the products of succinate-linked reduction of pyridine nucleotide. J Biol Chem. 236:1534–1543.

Chénais B, Morjani H, Drapier JC. 2002. Impact of endogenous nitric oxide on microglial cell energy metabolism and labile iron pool. J Neurochem. 81:615–623.

Cooper CE. 2002. Nitric oxide and cytochrome oxidase: substrate, inhibitor or effector? Trends Biochem Sci. 27:33–39.

Csordás G, Hajnóczky G. 2009. SR/ER-mitochondrial local communication: calcium and ROS. Biochim Biophys Acta. 1787:1352–1362.

Das AM, Harris DA. 1990. Intracellular calcium as a regulator of the mitochondrial ATP synthase in cultured cardiomyocytes. Biochem Soc Trans. 18:554–555.

Eastabrook RW. 1967. Mitochondrial respiratory control and the polarographic measurement of ADP:O ratio. Methods Enzymol. 10:41–47.

Emaus RD, Grunwald R, LeMasters JJ. 1986. Rhodamine 123 as a probe of transmembrane potential in isolated rat-liver mitochondria: spectral and metabolic properties. Biochim Biophys Acta. 950:436–448.

Feissner RF, Skalska J, Gaum WE, Sheu SS. 2009. Crosstalk signaling between mitochondrial Ca^{2+} and ROS. Front Biosci. 14:1197–1218.

Giuffrè A, Sarti P, D'Itri E, Buse G, Soulimane T, Brunori M. 1996. On the mechanism of inhibition of cytochrome c oxidase by nitric oxide. J Biol Chem. 271(52):33404–33408.

Gogvadze V, Walter PB, Ames BN. 2002. Fe(2 +) induces a transient Ca(2 +) release from rat liver mitochondria. Arch Biochem Biophys. 398:198–202.

Gorman AC, Thomas MV. 1978. Changes in the intracellular concentaration of free calcium ions in a pace-marker neurine, measured with the metallochronic indicator dye arsenazo III. J Physiol. 275:357–376.

Graier WF, Frieden M, Malli R. 2007. Mitochondria and Ca(2 +) signaling: old guests, new functions. Pflugers Arch. 455:375–396.

Grivennikova VG, Kotlyar AB, Karliner JS, Cecchini G, Vinogradov AD. 2007. Redox-dependent change of nucleotide affinity to the active site of the mammalian complex I. Biochemistry. 46:10971–10978.

Hansford RG, Zorov D. 1998. Role of mitochondrial calcium transport in the control of substrate oxidation. Mol Cell Biochem. 184:359–369.

Harley A, Cooper JM, Schapira AH. 1993. Iron induced oxidative stress and mitochondrial dysfunction: relevance to Parkinson's disease. Brain Res. 12:349–353.

Hulsmann WC, Bethlem J, Meijer AE, Fleury P, Schellens JP. 1967. Myopathy with abnormal structure and function of muscle mitochondria. J Neurol Neurosurg Psychiatry. 30:519–525.

Kanai AJ, Pearce LL, Clemens PR, Birder LA, VanBibber MM, Choi SY, de Groat WC, Peterson J. 2001. Identification of a neuronal nitric oxide synthase in isolated cardiac mitochondria using electrochemical detection. Proc Natl Acad Sci USA. 98:14126–14131.

Kim M, Hong M, Song E. 2009. Changes in cytochrome c oxidase and NO in rat lung mitochondria following iron overload. Animal Cells Systems. 13:105–112.

Kim M, Kim J, Cheon C-I, Cho DH, Park JH, Kim KI, Lee KY, Song E. 2008. Increased expression of the F_1Fo ATP synthase in response to iron in heart mitochondria. BMB Reports. 41:153–157.

Kolb JP, Paul-Eugene N, Damais C, Yamaoka K, Drapier JC, Dugas B. 1994. Interleukin-4 stimulates cGMP production by IFN-gamma-activated human monocytes. Involvement of the nitric oxide synthase pathway. J Biol Chem. 269:9811–9816.

Lehninger AL. 1970. Mitochondria and calcium ion transport. Biochem J. 119:129–138.

Lesnefsky EJ. 1994. Tissue iron overload and mechanisms of iron-catalyzed oxidative injury. Adv Exp Med Biol. 366:129–146.

Levi S, Luzzago A, Cesareni G, Cozzi A, Franceschinelli F, Albertini A, Arosio P. 1988. Mechanism of ferritin iron uptake: activity of the H-chain and deletion mapping of the ferro-oxidase site. A study of iron uptake and ferro-oxidase activity of human liver, recombinant H-chain ferritins, and of two H-chain deletion mutants. J Biol Chem. 263:18086–18092.

Levi S, Rovida E. 2009. The role of iron in mitochondrial function. Biochim Biophys Acta. 1790:629–636.

Lill R, Dutkiewicz R, Elsässer HP, Hausmann A, Netz DJ, Pierik AJ, Stehling O, Urzica E, Mühlenhoff U. 2006. Mechanisms of iron-sulfur protein maturation in mitochondria, cytosol and nucleus of eukaryotes. Biochim Biophys Acta. 1763:652–667.

Link G, Saada A, Pinson A, Konijn AM, Hershko C. 1998. Mitochondrial respiratory enzymes are a major target of iron toxicity in rat heart cells. J Lab Clin Med. 131:466–474.

Liu T, O'Rourke B. 2009. Regulation of mitochondrial Ca^{2+} and its effects on energetics and redox balance in normal and failing heart. J Bioenerg Biomembr. 41:127–132.

Lundin A, Thore A. 1975. Analytical information obtainable by evaluation of the time course of firefly bioluminescence in the assay of ATP. Anal Biochem. 66:47–63.

Machida K, Tanaka T. 1999. Farnesol-induced generation of reactive oxygen species dependent on mitochondrial transmembrane potential hyperpolarization mediated by F(0)F(1)-ATPase in yeast. FEBS Lett. 462:108–112.

Mao P, Ardeshiri A, Jacks R, Yang S, Hurn PD, Alkayed NJ. 2007. Mitochondrial mechanism of neuroprotection by CART. Eur J Neurosc. 26:624–632.

Masini A, Trenti T, Ceccarelli D, Muscatello U. 1987. The effect of a ferric iron complex on isolated rat liver mitochondria. III. Mechanistic aspects of iron induced calcium efflux. Biochim Biophys Acta. 891:150–156.

Muñoz M, Villar I, García-Erce JA. 2009. An update on iron physiology. World J Gastroenterol. 15:4617–4626.

Napier I, Ponka P, Richardson DR. 2005. Iron trafficking in the mitochondrion: novel pathways revealed by disease. Blood. 105:1867–1874.

Pande SV, Blanchaer MC. 1971. Reversible inhibition of mitochondrial adenosine diphosphate phosphorylation by long chain acyl coenzyme A esters. J Biol Chem. 246:402–411.

Pearce LL, Martinez-Bosch S, Manzano EL, Winnica DE, Epperly MW, Peterson J. 2009. The resistance of electron-transport chain Fe-S clusters to oxidative damage during the reaction of peroxynitrite with mitochondrial complex II and rat-heart pericardium. Nitric Oxide. 20:135–142.

Richardson DR, Lok HC. 2008. The nitric oxide-iron interplay in mammalian cells: transport and storage of dinitrosyl iron complexes. Biochim Biophys Acta. 1780:638–651.

Romslo I. 1975. Energy-dependent accumulation of iron by isolated rat liver mitochondria. IV. Relationship to the energy state of the mitochondria. Biochim Biophys Acta. 387:69–79.

Romslo I, Flatmark T. 1973. Energy-dependent accumulation of iron by isolated rat liver mitochondria. II. Relationship to the active transport of Ca^{2+}. Biochim Biophys Acta. 325:38–46.

Rouault TA, Tong WH. 2005. Iron-sulphur cluster biogenesis and mitochondrial iron homeostasis. Nat Rev Mol Cell Biol. 6:345–351.

Territo PR, Mootha VK, French SA, Balaban RS. 2000. Ca(2+) activation of heart mitochondrial oxidative phosphorylation: role of the F(0)/F(1)-ATPase. Am J Physiol Cell Physiol. 278:C423–435.

Valkonen M, Kuusi T. 1997. Spectrophotometric assay for total peroxyl radical-trapping antioxidant potential in human serum. J Lipid Res. 38:823–833.

Vatassery GT. 2004. Impairment of brain mitochondrial oxidative phosphorylation accompanying vitamin E oxidation induced by iron or reactive nitrogen species: a selective review. Neurochem Res. 29:1951–1959.

Vinogradov AD, Grivennikova VG. 2005. Generation of superoxide-radical by the NADH:Ubuquinone oxidoreductase of heart mitochondria. Biochemistry (Moscow) 70:120–127.

Walter PB, Knutson MD, Paler-Martinez A, Lee S, Xu Y, Viteri FE, Ames BN. 2002. Iron deficiency and iron excess damage mitochondria and mitochondrial DNA in rats. Proc Natl Acad Sci USA. 99:2264–2269.

Watts RN, Hawkins C, Ponka P, Richardson DR. 2006. Nitrogen monoxide (NO)-mediated iron release from cells is linked to NO-induced glutathione efflux via multidrug resistance-associated protein. Proc Natl Acad Sci USA. 103:7670–7675.

Ying W. 2008. NAD+/NADH and NADP+/NADPH in cellular functions and cell death: regulation and biological consequences. Antioxid Redox Signal. 10:179–206.